Hyperinflammation in Chronic Granulomatous Disease leads to impairment of hematopoietic stem cell functions

Maren Weisser, PhD[a], Uta M. Demel, MSc[b,c], Stefan Stein, PhD[a], Linping Chen-Wichmann, PhD[a1], Fabien Touzot, MD, PhD[d,e], Giorgia Santilli, PhD[f], Stefanie Sujer, MSc[b], Christian Brendel, PhD[a2], Ulrich Siler, PhD[g], Marina Cavazzana, MD, PhD[d,e], Adrian J. Thrasher, MD, PhD[f], Janine Reichenbach, MD[g], Marieke A.G. Essers, PhD[b,c], Joachim Schwäble, MD[a,h†3] and Manuel Grez, PhD[a†°]

[a]Institute for Tumor Biology and Experimental Therapy, Georg-Speyer-Haus, Frankfurt, Germany; [b]Junior Research Group 'Hematopoietic Stem Cells and Stress', German Cancer Research Center (DKFZ), INF280, Heidelberg, Germany; [c]Heidelberg Institute for Stem Cell Technology and Experimental Medicine (HI-STEM), INF280, Heidelberg, Germany; [d]Biotherapy Department, Necker Children's Hospital, Assistance Publique-Hôpitaux de Paris, Paris, France; [e]Paris Descartes – Sorbonne Paris Cité University, Imagine Institute, Paris, France; [f]Section of Molecular and Cellular Immunology, UCL Institute of Child Health, London, United Kingdom; [g]Division of Immunology, University Children's Hospital, and Children's Research Centre Zürich, Switzerland; [h]Department of Medicine, Hematology/Oncology, Goethe University, Frankfurt am Main, Germany

[1]Present address: Experimental Cell Therapy and Hematology, Department of Transfusion Medicine, Cell Therapy and Haemostaseology, Ludwig Maximilian University Hospital Munich, Germany

[2]Present address: Division of Hematology/Oncology, Boston Children's Hospital, Boston, MA, USA

[3]Present address: German Red Cross Blood Donor Service Baden-Württemberg – Hessen and Institute for Transfusion Medicine and Immunohematology of the Goethe University, Frankfurt, Germany

° Corresponding author:
Manuel Grez, PhD
Institute for Tumor Biology and Experimental Therapy
Georg-Speyer-Haus, Paul-Ehrlich-Str. 42-44
60596 Frankfurt, Germany
Tel: +49 69 63395-113; Fax: +49 69 63395-297
Email: grez@gsh.uni-frankfurt.de

†Equal contribution

This study work was supported by grants from the Deutsche Forschungsgemeinschaft (SFB815), the European Union (FP7 integrated project NET4CGD), the Wellcome Trust and the LOEWE Center for Cell and Gene Therapy Frankfurt funded by the Hessische Ministerium für Wissenschaft und Kunst (HMWK; funding reference numbers: III L 4-518/17.004 (2010) and III L 5- 518/17.004 (2013)). UD, SSu, and MAGE are supported by the SFB873, funded by the Deutsche Forschungsgemeinschaft (DFG) and the Dietmar Hopp Foundation. JR and US were funded by the Gebert Rüf Stiftung, programme "Rare Diseases – New approaches" (grant no. GRS-046/10, JR), the Zurich Centre for Integrative Human Physiology (ZIHP, JR), and by the Ettore e Valeria Rossi Foundation. The Georg-Speyer-Haus is funded jointly by the German Federal Ministry of Health (BMG) and the Hessische Ministerium für Wissenschaft und Kunst.

Conflict-of-interest disclosure: The authors declare no competing financial interests.

Abstract

Background: Defects in the phagocytic NADPH oxidase 2 (NOX2) function cause chronic granulomatous disease (CGD), a primary immunodeficiency characterized by dysfunctional microbicidal activity and chronic inflammation.

Objective: To study the effect of chronic inflammation on the hematopoietic compartment in patients and mice with the X-linked form of CGD (X-CGD).

Methods: We used immunostaining and functional analyses to study the hematopoietic compartment in CGD.

Results: Analysis of bone marrow (BM) cells from X-CGD patients and mice revealed a dysregulated hematopoiesis characterized by increased numbers of hematopoietic progenitors (HPCs) at the expense of repopulating hematopoietic stem cells (HSCs). In X-CGD patients there was a clear reduction in the proportion of HSCs in BM and peripheral blood and they were also more rapidly exhausted after *in vitro* culture. In X-CGD mice, increased cycling of HSCs, expansion of HPCs and impaired long-term engraftment capacity were found to be associated with high concentrations of proinflammatory cytokines, including interleukin 1 beta (IL-1β). Treatment of wild-type mice with IL-1β induced enhanced cell cycle entry of HSCs, expansion of HPCs and defects in long-term engraftment, mimicking the effects observed in X-CGD mice. Inhibition of cytokine signaling in X-CGD mice reduced HPC numbers but had only minor effects on the repopulating ability of HSCs.

Conclusions: Persistent chronic inflammation in CGD is associated with hematopoietic proliferative stress leading to a decrease in the functional activity of HSCs. Our observations have clinical implications for the development of successful autologous cell therapy approaches.

Key messages:

- Chronic inflammation in X-CGD is associated with dysregulated hematopoiesis and impaired hematopoietic stem cell activity.

- IL-1β is increased in X-CGD and induces cycling of hematopoietic stem cells leading to a decrease in HSC function and increased numbers of hematopoietic progenitors with limited repopulating capacities.

Capsule Summary

Inflammation in X-CGD is associated with increased numbers of HPCs and functionally impaired HSCs as a result of increased cytokine production, including IL-1β.

Key Words

Chronic Granulomatous Disease, hyperinflammation, hematopoietic stem cell, dysfunctional hematopoiesis, competitive repopulation assay, engraftment defect, cell cycle, IL-1β, Anakinra, gene therapy

Abbreviations

BM: bone marrow
CFU: colony forming unit
CGD: Chronic Granulomatous Disease
CMP/MEP/GMP: common myeloid progenitor/megakaryocyte-erythroid progenitor/granulocyte-macrophage progenitor
CRU: competitive repopulating unit
HC: healthy control
HSC/HPC: hematopoietic stem cell / hematopoietic progenitor cell
NADPH: nicotinamide adenine dinucleotide phosphate
NOX2: NADPH oxidase 2
PB: peripheral blood
WT: wild type
X-CGD: X-linked CGD

Introduction

Chronic Granulomatous Disease (CGD) is a rare inherited primary immunodeficiency characterized by defective antimicrobicidal activity of phagocytes, resulting in increased susceptibility to recurrent and life-threatening infections.[1-6] In addition, CGD patients often display augmented inflammatory responses, even in the absence of infectious agents (sterile inflammation), leading to granuloma formation and inflammatory bowel disease.[7-10] Approximately two thirds of all CGD patients have mutations within the X-linked *CYBB* gene (X-CGD), encoding the gp91^{phox} subunit of NOX2. X-CGD mice faithfully reproduce the pathology observed in X-CGD patients.[7,11]

CGD can be cured by allogeneic HSC transplantation, which has been particularly successful in patients with a fully HLA-matched donor in combination with reduced-intensity conditioning.[12,13] Despite the use of advanced HSC transplantation protocols, cases of low donor chimerism, graft-versus-host disease and graft rejection have been observed.[14-16] Thus, for those patients without suitable HSC donors and for those in critical health conditions, alternative treatment options beyond the standard of care are still required. The transplantation of autologous gene-modified cells is an alternative for the treatment of CGD, and has been implemented predominantly in X-CGD patients.[17-20] These clinical trials have provided evidence that gene therapy can offer significant clinical benefit to CGD patients. However, most of the patients lacked significant long-term engraftment of transduced cells.[21,22] Although many factors may have influenced the engraftment potential of CD34$^+$ cells during cell processing, alterations in numbers and/or fitness of HSCs in the CGD inflammatory background could also contribute to the engraftment deficit. We therefore analyzed the influence of chronic inflammation on the HSC compartment in X-CGD. We found a profound defect in HSC content and/or activity in the bone marrow (BM) of both X-CGD patients and mice.

The hematopoietic defects observed in X-CGD mice were mainly mediated by IL-1β and inhibition of IL-1β signaling suppressed HPC expansion in X-CGD mice but did not revert the functional defects in HSC activity.

Thus, chronic inflammation in CGD leads to a dysregulated hematopoietic homeostasis. Our findings may not be limited to CGD, but may also be relevant to other pathologies with sustained chronic inflammation and autoinflammatory processes.[23-27]

Methods

Patient material

BM and G-CSF mobilized peripheral blood (PB) mononuclear cells were obtained from X-CGD patients (BM: n = 3, median 5.5 years old, range 0.7-8 years; PB: n=4, median: 10 years old, range 4-17 years) and healthy controls (BM: n = 4, median 11 years old, range: 3-14 years; PB: n=4, median 29, range 25-37 years) after informed consent and approval by the local ethic committee.

Mice

B6.129S6-*Cybb*^{tm1Din}/J (X-CGD mice, CD45.2), C57BL/6J (WT mice, CD45.2) and B6.SJL-*Ptprc*^{a} *Pepc*^{b}/BoyJ (CD45.1) mice were obtained from Charles River Laboratories (Sulzfeld, Germany). Health monitoring was conducted regularly by MFD Diagnostics (Wendelsheim, Germany) according to Federation for Laboratory Animal Science Associations guidelines. Animals with overt infections were not included in the study. Male littermates were used for experiments unless stated otherwise. B6.Cg MyD88^{tm1Aki} mice (MyD88-deficient mice)[28] were bred at the Animal Facility of the German Cancer Research Center. Animal experiments were approved by the regional council (Regierungspräsidium Darmstadt, Germany).

166 **Hematopoietic Stem Cell assays and Cytokine Arrays**

167 All assays including cell isolation, analysis and sorting, HSC assays, cell cycle analysis,
168 cytokine stimulation experiments, lentiviral transductions, transplantation assays, competitive
169 repopulation assays and cytokine arrays were done according to standard protocols. Detailed
170 methods are provided in the Supplementary Material section in this article's Online
171 Repository.

172 **Statistical Analysis**

173 Statistical significances were calculated by unpaired two-tailed t-tests (Fig 1-2, 4A, C-D, F-G,
174 5C), one-factorial ANOVA with Dunnet's Multiple Comparison Test (Fig 4B), two-factorial
175 ANOVA with Bonferroni posttests (Fig 3A, C, 4E, 5A-B) and three-factorial ANOVA (Fig
176 4H). CRU frequency was calculated with L-Calc Limiting Dilution Analysis Software
177 (StemSoft, Version 1.1). Overall test for differences in CRU frequencies between X-CGD and
178 WT was performed with ELDA: Extreme Limiting Dilution Analysis
179 (http://bioinf.wehi.edu.au/software/elda/index.html). Scatter plots indicate mean ± SD. Bar
180 diagrams show mean + SD. * $p < 0.05$, ** $p < 0.01$, *** $p < 0.001$.

181 ## Results

182 **Increased numbers of hematopoietic progenitors in X-CGD mice**

183 We analyzed the hematopoietic compartment of X-CGD mice and found significantly
184 ($p < 0.05$-0.01) increased levels of LSK (Lin^- $Sca\text{-}1^+$ $c\text{-}Kit^+$) cells, myeloid progenitors,
185 common myeloid progenitors (CMPs) and granulocyte-monocyte progenitors (GMPs) in the
186 BM, whereas the percentages of LSK SLAM (Lin^- $Sca\text{-}1^+$ $c\text{-}Kit^+$ $CD150^+$ $CD48^-$), lineage
187 negative (Lin^-) and megakaryocyte-erythroid progenitors (MEPs) cells were unchanged (Fig
188 1, *A*-*E* and see Fig E1, *A*-*B*, in the Online Repository and data not shown). BM cells from X-
189 CGD animals generated higher numbers of colonies derived from granulocyte-monocyte-
190 progenitors (CFU-GM) than cells from WT mice (see Fig E1, *C*, in the Online Repository).

LSK cells and the number of CFUs derived from spleen and PB were higher in X-CGD mice (Fig 1, *F-G*, and see Fig E1, *D* in the Online Repository). Cell cycle analysis revealed that the frequency of quiescent HSCs in X-CGD BM was significantly ($p < 0.01$) reduced compared to WT (Fig 1, *H-I*), suggesting an increase in the percentage of actively cycling HSCs in X-CGD animals.

Reduced numbers of HSCs in human X-CGD BM and mobilized peripheral blood

We analyzed BM from X-CGD patients (n = 3) versus age-matched healthy controls (n = 4). We found a significant increase in the proportion of committed progenitors ($CD34^+ Lin^- CD38^+$) in X-CGD BM at the expense of HSCs ($CD34^+ Lin^- CD38^-$)(Fig 2, *A-B* and see Fig E2, *A*, in the Online Repository). Moreover, we found a shift in the balance of progenitors with the tendency towards less CMPs and MEPs and more GMPs in X-CGD BM when compared to healthy controls (Fig E2, *B-D*, in the Online Repository). Analysis of G-CSF mobilized PB mononuclear cells obtained from X-CGD patients (n = 3) revealed a pronounced reduction in the proportion of primitive HSCs ($CD34^+ CD38^- CD90^+$) and early progenitors ($CD34^+ CD38^-$) compared to healthy donors (n = 3) (Fig 2, *C-D* and see Fig E3 in the Online Repository). Isolated PB $CD34^+CD38^{dim}CD90^+$ cells from healthy donors and X-CGD patients were cultured in the presence of early-acting cytokines for 4 days, thus resembling the conditions used in gene therapy settings. At day 4 HSCs and multipotent progenitors accounted for half of the population in the sample derived from healthy donors, while HSCs and MPPs derived from X-CGD patients were rapidly exhausted under these conditions (Fig 2, *E*). More than 85% of the X-CGD cells remaining in the culture were $CD38^+$ late progenitors, a cell population with restricted engraftment capacities. These observations indicate that the alterations in the HSC/HPC pool observed in X-CGD mice are reciprocated in X-CGD patients and suggest a common underlying aetiology.

Impaired competitive repopulating ability of HSCs derived from X-CGD mice

To assess the fitness of HSCs/HPCs we monitored the production of CFUs from BM long-term cultures derived from X-CGD or WT animals after 4, 8 or 12 weeks of culture. Cells from X-CGD BM produced a significantly higher number of CFUs than WT cells after 4 weeks of culture, consistent with the elevated LSK cell count (Fig 3, *A*). However, after 12 weeks culture the number of X-CGD-derived CFUs was reduced compared to WT, indicating an accelerated exhaustion of the HSC pool. We also analyzed the self-renewal capability of HSCs *in vivo* by exposing mice to serial cytotoxic injury through repeated 5-fluorouracil (5-FU) dosing. This treatment depletes replicating cells and promotes activation of formerly quiescent HSCs. In this assay, the survival of X-CGD mice was impaired compared to WT animals, again suggesting early exhaustion of HSCs (Fig 3, *B*).

Next, we compared the capability of X-CGD and WT HSCs to reconstitute hematopoiesis in transplanted recipients. Lin^- cells from either mouse group were differentially labeled using eGFP- or tBFP-encoding lentiviral vectors and equal numbers of gene-marked cells were mixed and transplanted into recipient mice. PB analyses at 2, 4, 8, 12 and 18 weeks showed that in the first weeks after transplantation, the frequency of gene-marked X-CGD cells in PB was higher compared to WT cells. However, gene-marked X-CGD cells were outcompeted by their WT counterparts from week 4 onwards, suggesting a lower frequency of long-term repopulating cells in the X-CGD samples (Fig 3, *C*).

Lastly, we estimated the absolute number of cells with myeloid and lymphoid reconstitution potential in the BM of WT and X-CGD mice by a limiting dilution competitive repopulating unit (CRU) assay with LSK SLAM cells. Short-term repopulation analysis after 4 weeks resulted in similar CRU frequencies in both mouse groups. Upon 8 weeks and 16 weeks after transplantation X-CGD HSCs displayed a reduced (1.8-fold, $p = 0.079$) multilineage contribution to the PB of primary hosts compared to WT HSCs (Fig 3, *D*). Subsequently, isolated HSCs from animals transplanted with 50 and 250 LSK SLAM cells were used for

secondary BM transplantation. Sixteen weeks after secondary transplantation 79% (11/14) of the recipient animals injected with WT BM, but only 22% (4/18) of hosts receiving X-CGD BM showed successful multilineage repopulation in the PB (Fig 3, *E*). Taken together, our *in vitro* and *in vivo* experiments reveal a reduced potential of primitive HSCs derived from X-CGD mice to reconstitute long-term hematopoiesis.

No intrinsic defect in HSCs derived from X-CGD mice

To study whether the defects observed for X-CGD HSCs were intrinsic or acquired over time, we analyzed fetal liver HSCs/HPCs. The composition of the fetal liver HSCs/HPCs was comparable for X-CGD and WT mice (see Fig E4, *A*, in the Online Repository). Competitive transplantations were performed with Lin^- fetal liver cells from X-CGD and WT littermates. X-CGD fetal liver HSCs/HPCs were capable of engrafting and maintaining multilineage hematopoiesis to the same extent as WT cells (see Fig E4, *B*, in the Online Repository). This indicates that the observed deficits in long-term repopulation abilities of adult X-CGD HSCs are indeed acquired over time. As alterations in the BM microenvironment might be involved in the development of the long-term repopulation defect, we performed transplantations of WT (CD45.1) Lin^- cells into WT (CD45.2) and X-CGD recipient mice. No significant differences in engraftment and chimerism, response to 5-FU challenge or hematopoietic reconstitution in secondary transplanted animals between both groups were observed (see Fig E4, *C-E*, in the Online Repository).

Increased levels of proinflammatory cytokines in the BM of X-CGD animals

In light of the established proinflammatory phenotype associated with CGD we screened BM fluid from WT and X-CGD mice for chemokine and cytokine levels using protein arrays. A high proportion of cytokines/chemokines (17/40) was significantly ($p < 0.05$) upregulated in the lavage from X-CGD BM (see Fig E5, *A* and Table E1 in the Online Repository). The

levels of C-X-C motif chemokine (CXCL) 9, CXCL10, CXCL13, C-C motif chemokine 5 (CCL5) and IL-1β were increased between 1.8 and 7.8-fold compared to WT. Likewise, the levels of other cytokines known to modulate HSC homeostasis were also altered (M-CSF, IL-3, IL-1α, TIMP-1), although to a minor extend. Quantification of IL-1β by ELISA revealed a 1.5-fold higher concentration in X-CGD compared to BM lavages from WT mice (Fig 4, *A*).

Next we analyzed the effects of the cytokines and chemokines IL-1β, CXCL10, CCL5 and CXCL9 on LSK cell proliferation *in vitro*. The stimulation of WT Lin^- cells with CXCL10 induced a modest increase in the frequency of LSK cells, while CCL5 and CXCL9 had no effect (see Fig E5, *B*, in the Online Repository). Addition of IL-1β was sufficient to expand the LSK cell pool 2.3- to 2.4-fold (Fig 4, *B*). Moreover, upon injection of IL-1β we observed a significant ($p < 0.01$) increase in the proportion of LSK cells in the BM of WT animals (Fig 4, *C*). This was associated with cell cycle activation of HSCs, as shown by increased BrdU incorporation into LSK $CD150^+$ $CD48^-$ $CD34^-$ cells (Fig 4, *D*) and a decrease in the frequency of quiescent HSCs (Fig 4, *E*).

Most likely, the effects of IL-1β are mediated by IL-1β binding to its receptor and subsequent activation of downstream signals, as the effects of IL-1β on HSC activation were absent in mice lacking MyD88, an essential adaptor molecule of IL-1β signaling (Fig 4, *E*). In addition, treatment of WT mice with IL-1β resulted in a higher content of colony forming cells in the bone marrow and increased LSK cell frequencies in the spleen, thus reproducing faithfully the phenotype observed in X-CGD animals (Fig 4, *F-G*). Lastly, we performed competitive transplantation assays with a mixture of bone marrow cells containing $2x10^6$ mononuclear cells obtained from animals treated with IL1-β and PBS. In all transplanted animals the engraftment of cells derived from the IL-1β-treated animals was inferior to the engraftment of control cells (Fig 4, *H*). This data shows conclusively that IL-1β has detrimental effects on the fitness of the HSC pool.

Blocking inflammatory signals partially reverts the hematopoietic dysfunction in X-CGD mice

We treated 3-4 weeks old X-CGD and WT mice intraperitoneally with the IL-1β receptor antagonist Anakinra or PBS for 14-16 days. Anakinra treatment led to a decrease in the proportion of LSK cells in the BM ($p < 0.05$) and spleen of X-CGD but not WT mice and a decrease in the number of colony forming cells (CFCs) in peripheral blood (Fig 5, A-*B*, and see Fig E6 in the Online Repository). In addition, X-CGD mice were treated with the anti-inflammatory steroid dexamethasone alone or in combination with Anakinra for 14 days. Dexamethasone and dexamethasone + Anakinra led to a decrease in the proportion of LSK cells in the BM ($p < 0.05$) and in the spleen of X-CGD mice, although the later did not reach significance (Fig 5, *C-D*). Also the number of CFCs in the bone marrow of dexamethasone-treated animals was decreased (see Fig E6 in the Online Repository). The combined dexamethasone + Anakinra treatment reduced the IL-1β concentration in the bone lavages significantly (Fig 5, *E*). In competitive transplantation experiments 4,000 Lin^- BM cells from PBS-, Anakinra-, or dexamethasone- treated X-CGD mice (CD45.2) were transplanted together with 10^5 CD45.1 mononuclear cells in CD45.1 recipients. Analysis of BM and PB chimerism at 19 and 8 weeks after transplantation, respectively showed a slight improvement in engraftment of cells derived from the Anakinra- or dexamethasone-treated animals, although the difference to the recipients of PBS-treated controls did not reach significance (see Fig E6 in the Online Repository). Nevertheless multilineage engraftment was obtained in 8 out of 13 recipients transplanted with cells from the dexamethasone-treated group, while only 4 out of 10 recipients of the PBS-treated group showed tri-lineage engraftment above 0.1%.

In summary our findings suggest that pro-inflammatory cytokines are responsible for the increased HPC pool and dysfunctional HSCs in X-CGD (Fig 5, *F*).

Discussion

Our data show that hematopoiesis is dysregulated in X-CGD. Both the quality and quantity of HSCs are affected, as demonstrated by the low proportion of primitive HSCs/HPCs present in BM cells from X-CGD patients and the low repopulation efficiency of murine X-CGD BM cells. Our observations add to the recent report by Panch et al., demonstrating a significant reduction in the number of G-CSF mobilized $CD34^+$ cells in X-CGD patients.[29] Similar to our findings, the deficit in $CD34^+$ mobilization was directly associated with parameters linked to inflammation.

Inflammation is known to promote HSC proliferation and orchestrates HSC/HPC egress to the blood stream via a variety of mechanisms.[30-36] Inflammatory signals lead to augmented NF-κB activity, transcription of proinflammatory cytokines and activation of the inflammasome resulting in caspase-1-dependent secretion of the proinflammatory cytokines IL-1β and IL-18.[37-39] In CGD patients, increased activity of caspase-1 and elevated release of IL-1β and other proinflammatory cytokines by activated mononuclear cells contributes to dysregulated inflammatory responses, even in the absence of clinical infection.[7-9,40-48] In view of the compelling evidence linking inflammation with defects in HSCs, it is not surprising that similar defects are observed in the HSC compartment of CGD patients and mice.

We found that a series of proinflammatory mediators were upregulated in samples derived from BM of X-CGD animals partially overlapping with those previously identified in a cDNA microarray analysis on isolated X-CGD monocytes.[49] In particular, we found increased IL-1β levels in BM of X-CGD mice, a pleiotropic proinflammatory modulator of other cytokines, adhesion molecules and enzymes which also influences hematopoietic cell differentiation.[50,51]

IL-1β activates HSCs, which are known to express IL-1 receptors[52] and induces HSCs to exit from quiescence. Cell cycle induction by IL-1β has been previously demonstrated in human $CD34^+$ $CD38^-$ acute myeloid leukemia cells, leading to the downregulation of the cell cycle inhibitor p21, impaired self-renewal and reduced reconstitution potential.[53] Similarly, reduced repopulation capacity has been shown for LSK cells upon treatment of mice with IL-1α, which also triggers signaling through the IL-1 receptor.[54]

We propose a model, in which a functional defect in X-CGD HSCs develops over time due to persistent exposure of HSCs/HPCs to inflammatory cytokines and chemokines. Chronic inflammation has been linked to enhanced cell cycle entry of HSCs, impaired repopulation ability and HSC exhaustion.[35,36,55] Treatment of CGD patients with the IL-1 receptor antagonist Anakinra led to suppression of inflammation-related colitis in one study but only partial responses in others.[41,46,56] In our studies, treatment of X-CGD mice with Anakinra alone resulted in reconstitution of HPCs levels and in combination with dexamethasone to a reduction of IL-1β secretion. Thus, proactive treatment of CGD patients with anti-inflammatory drugs might therefore reduce chronic sterile inflammation in CGD and could also have an impact on the quantity of HSCs available for autologous gene therapy. In terms of clinical practice, our results implies that large numbers of CD34+ cells need to be collected for genetic modification from X-CGD patients undergoing gene therapy. Furthermore the decrease in the percentage of $CD34^+/CD38^-$ in the peripheral blood of G-CSF-mobilized X-CGD patients and the almost complete loss of primitive HSCs ($CD34^+CD38^-CD90^+$ cells) after a 4 days culture period in the presence of cytokines raises concerns as to current expansion protocols and warrants the development of alternative mobilization and cell culture strategies to avoid premature cell differentiation and lastly graft failure. Finally, anti-inflammatory treatment of X-CGD patients prior to collection of $CD34^+$ cells might improve the ratio between HSCs and progenitors in the graft and consequently may increase the proportion of transduced cells with engrafting potential. Ultimately these measurements may

lead to successful engraftment of gene corrected cells in CGD patients enrolled in a gene therapy program.

Acknowledgments

We thank Hana Kunkel, Tefik Merovci (both GSH, Frankfurt, Germany), Maeva Joigneaux and Laure Caccavelli (both Necker Children's Hospital, Paris, France) and Christian Brandts and The Duy Nguyen (both University Hospital, Frankfurt, Germany) for technical help and reagents. Thanks also to Kerstin Kaufmann and Hind Medyouf (both GSH, Frankfurt, Germany) and Christian Wichmann (Ludwig Maximilian University Hospital, Munich, Germany) for advice and critical reading of the manuscript. We thank Gaby Schneider (Institute for Mathematics, Goethe University Frankfurt, Germany) for her help with the statistical analyses.

References

1. Roos D. The genetic basis of chronic granulomatous disease. Immunol Rev 1994; 138:121-57.

2. Segal AW. The NADPH oxidase and chronic granulomatous disease. Mol Med Today 1996; 2:129-35.

3. Segal BH, Leto TL, Gallin JI, Malech HL, Holland SM. Genetic, biochemical, and clinical features of chronic granulomatous disease. Medicine (Baltimore) 2000; 79:170-200.

4. Seger RA. Chronic granulomatous disease: recent advances in pathophysiology and treatment. Neth J Med 2010; 68:334-40.

5. Dinauer MC. Chronic granulomatous disease and other disorders of phagocyte function. Hematology Am Soc Hematol Educ Program 2005:89-95.

6. Bianchi M, Niemiec MJ, Siler U, Urban CF, Reichenbach J. Restoration of anti-Aspergillus defense by neutrophil extracellular traps in human chronic granulomatous disease after gene therapy is calprotectin-dependent. J Allergy Clin Immunol 2011; 127:1243-52 e7.

7. Morgenstern DE, Gifford MA, Li LL, Doerschuk CM, Dinauer MC. Absence of respiratory burst in X-linked chronic granulomatous disease mice leads to abnormalities in both host defense and inflammatory response to Aspergillus fumigatus. J Exp Med 1997; 185:207-18.

8. Rosenzweig SD. Inflammatory manifestations in chronic granulomatous disease (CGD). J Clin Immunol 2008; 28 Suppl 1:S67-72.

9. Schappi MG, Jaquet V, Belli DC, Krause KH. Hyperinflammation in chronic granulomatous disease and anti-inflammatory role of the phagocyte NADPH oxidase. Semin Immunopathol 2008; 30:255-71.

10. Magnani A, Brosselin P, Beaute J, de Vergnes N, Mouy R, Debre M, et al. Inflammatory manifestations in a single-center cohort of patients with chronic granulomatous disease. J Allergy Clin Immunol 2014; 134:655-62 e8.

410 11. Petersen JE, Hiran TS, Goebel WS, Johnson C, Murphy RC, Azmi FH, et al.
411 Enhanced cutaneous inflammatory reactions to Aspergillus fumigatus in a murine model of
412 chronic granulomatous disease. J Invest Dermatol 2002; 118:424-9.
413 12. Seger RA. Modern management of chronic granulomatous disease. Br J Haematol
414 2008; 140:255-66.
415 13. Gungor T, Teira P, Slatter M, Stussi G, Stepensky P, Moshous D, et al. Reduced-
416 intensity conditioning and HLA-matched haemopoietic stem-cell transplantation in patients
417 with chronic granulomatous disease: a prospective multicentre study. Lancet 2013; 383:436-
418 48.
419 14. Oshrine B, Morsheimer M, Heimall J, Bunin N. Reduced-Intensity Conditioning for
420 Hematopoietic Cell Transplantation of Chronic Granulomatous Disease. Pediatr Blood Cancer
421 2015; 62:359-61.
422 15. Ahlin A, Fasth A. Chronic granulomatous disease - conventional treatment vs.
423 hematopoietic stem cell transplantation: an update. Curr Opin Hematol 2015; 22:41-5.
424 16. Cole T, Pearce MS, Cant AJ, Cale CM, Goldblatt D, Gennery AR. Clinical outcome in
425 children with chronic granulomatous disease managed conservatively or with hematopoietic
426 stem cell transplantation. J Allergy Clin Immunol 2013; 132:1150-5.
427 17. Bianchi M, Hakkim A, Brinkmann V, Siler U, Seger RA, Zychlinsky A, et al.
428 Restoration of NET formation by gene therapy in CGD controls aspergillosis. Blood 2009;
429 114:2619-22.
430 18. Kang EM, Choi U, Theobald N, Linton G, Long Priel DA, Kuhns D, et al. Retrovirus
431 gene therapy for X-linked chronic granulomatous disease can achieve stable long-term
432 correction of oxidase activity in peripheral blood neutrophils. Blood 2010; 115:783-91.
433 19. Kang HJ, Bartholomae CC, Paruzynski A, Arens A, Kim S, Yu SS, et al. Retroviral
434 gene therapy for X-linked chronic granulomatous disease: results from phase I/II trial. Mol
435 Ther 2011; 19:2092-101.

436 20. Ott MG, Schmidt M, Schwarzwaelder K, Stein S, Siler U, Koehl U, et al. Correction
437 of X-linked chronic granulomatous disease by gene therapy, augmented by insertional
438 activation of MDS1-EVI1, PRDM16 or SETBP1. Nat Med 2006; 12:401-9.
439 21. Stein S, Ott MG, Schultze-Strasser S, Jauch A, Burwinkel B, Kinner A, et al. Genomic
440 instability and myelodysplasia with monosomy 7 consequent to EVI1 activation after gene
441 therapy for chronic granulomatous disease. Nat Med 2010; 16:198-204.
442 22. Grez M, Reichenbach J, Schwable J, Seger R, Dinauer MC, Thrasher AJ. Gene
443 therapy of chronic granulomatous disease: the engraftment dilemma. Mol Ther 2011; 19:28-
444 35.
445 23. Feldman N, Rotter-Maskowitz A, Okun E. DAMPs as mediators of sterile
446 inflammation in aging-related pathologies. Ageing Res Rev 2015; Jan 29:doi:
447 10.1016/j.arr.2015.01.003. [Epub ahead of print].
448 24. Geiger H, Denkinger M, Schirmbeck R. Hematopoietic stem cell aging. Curr Opin
449 Immunol 2014; 29:86-92.
450 25. Sauce D, Larsen M, Fastenackels S, Pauchard M, Ait-Mohand H, Schneider L, et al.
451 HIV disease progression despite suppression of viral replication is associated with exhaustion
452 of lymphopoiesis. Blood 2011; 117:5142-51.
453 26. Makipour S, Kanapuru B, Ershler WB. Unexplained anemia in the elderly. Semin
454 Hematol 2008; 45:250-4.
455 27. Dinarello CA, Simon A, van der Meer JW. Treating inflammation by blocking
456 interleukin-1 in a broad spectrum of diseases. Nat Rev Drug Discov 2012; 11:633-52.
457 28. Adachi O, Kawai T, Takeda K, Matsumoto M, Tsutsui H, Sakagami M, et al. Targeted
458 disruption of the MyD88 gene results in loss of IL-1- and IL-18-mediated function. Immunity
459 1998; 9:143-50.
460 29. Panch SR, Yau YY, Kang EM, De Ravin SS, Malech HL, Leitman SF. Mobilization
461 characteristics and strategies to improve hematopoietic progenitor cell mobilization and

462 collection in patients with chronic granulomatous disease and severe combined
463 immunodeficiency. Transfusion 2015; 55:265-74.
464 30. Rodriguez S, Chora A, Goumnerov B, Mumaw C, Goebel WS, Fernandez L, et al.
465 Dysfunctional expansion of hematopoietic stem cells and block of myeloid differentiation in
466 lethal sepsis. Blood 2009; 114:4064-76.
467 31. Zhang P, Nelson S, Bagby GJ, Siggins R, 2nd, Shellito JE, Welsh DA. The lineage-c-
468 Kit+Sca-1+ cell response to Escherichia coli bacteremia in Balb/c mice. Stem Cells 2008;
469 26:1778-86.
470 32. Singh P, Yao Y, Weliver A, Broxmeyer HE, Hong SC, Chang CH. Vaccinia virus
471 infection modulates the hematopoietic cell compartments in the bone marrow. Stem Cells
472 2008; 26:1009-16.
473 33. Baldridge MT, King KY, Goodell MA. Inflammatory signals regulate hematopoietic
474 stem cells. Trends Immunol 2011; 32:57-65.
475 34. Griseri T, McKenzie BS, Schiering C, Powrie F. Dysregulated hematopoietic stem and
476 progenitor cell activity promotes interleukin-23-driven chronic intestinal inflammation.
477 Immunity 2012; 37:1116-29.
478 35. Essers MA, Offner S, Blanco-Bose WE, Waibler Z, Kalinke U, Duchosal MA, et al.
479 IFNalpha activates dormant haematopoietic stem cells in vivo. Nature 2009; 458:904-8.
480 36. Essers MA, Trumpp A. Targeting leukemic stem cells by breaking their dormancy.
481 Mol Oncol 2010; 4:443-50.
482 37. Chen GY, Nunez G. Sterile inflammation: sensing and reacting to damage. Nat Rev
483 Immunol 2010; 10:826-37.
484 38. Henao-Mejia J, Elinav E, Strowig T, Flavell RA. Inflammasomes: far beyond
485 inflammation. Nat Immunol 2012; 13:321-4.
486 39. Strowig T, Henao-Mejia J, Elinav E, Flavell R. Inflammasomes in health and disease.
487 Nature 2012; 481:278-86.

488 40. Brown JR, Goldblatt D, Buddle J, Morton L, Thrasher AJ. Diminished production of
489 anti-inflammatory mediators during neutrophil apoptosis and macrophage phagocytosis in
490 chronic granulomatous disease (CGD). J Leukoc Biol 2003; 73:591-9.
491 41. Meissner F, Seger RA, Moshous D, Fischer A, Reichenbach J, Zychlinsky A.
492 Inflammasome activation in NADPH oxidase defective mononuclear phagocytes from
493 patients with chronic granulomatous disease. Blood 2010; 116:1570-3.
494 42. van de Veerdonk FL, Smeekens SP, Joosten LA, Kullberg BJ, Dinarello CA, van der
495 Meer JW, et al. Reactive oxygen species-independent activation of the IL-1beta
496 inflammasome in cells from patients with chronic granulomatous disease. Proc Natl Acad Sci
497 U S A 2010; 107:3030-3.
498 43. Segal BH, Han W, Bushey JJ, Joo M, Bhatti Z, Feminella J, et al. NADPH oxidase
499 limits innate immune responses in the lungs in mice. PLoS One 2010; 5:e9631.
500 44. Rubartelli A. Redox control of NLRP3 inflammasome activation in health and disease.
501 J Leukoc Biol 2012; 92:951-8.
502 45. Zeng MY, Pham D, Bagaitkar J, Liu J, Otero K, Shan M, et al. An efferocytosis-
503 induced, IL-4-dependent macrophage-iNKT cell circuit suppresses sterile inflammation and is
504 defective in murine CGD. Blood 2013; 121:3473-83.
505 46. de Luca A, Smeekens SP, Casagrande A, Iannitti R, Conway KL, Gresnigt MS, et al.
506 IL-1 receptor blockade restores autophagy and reduces inflammation in chronic
507 granulomatous disease in mice and in humans. Proc Natl Acad Sci U S A 2014; 111:3526-31.
508 47. Baroja-Mazo A, Martin-Sanchez F, Gomez AI, Martinez CM, Amores-Iniesta J,
509 Compan V, et al. The NLRP3 inflammasome is released as a particulate danger signal that
510 amplifies the inflammatory response. Nat Immunol 2014; 15:738-48.
511 48. Geering B, Stoeckle C, Conus S, Simon HU. Living and dying for inflammation:
512 neutrophils, eosinophils, basophils. Trends Immunol 2013; 34:398-409.

513 49. Brown KL, Bylund J, MacDonald KL, Song-Zhao GX, Elliott MR, Falsafi R, et al.
514 ROS-deficient monocytes have aberrant gene expression that correlates with inflammatory
515 disorders of chronic granulomatous disease. Clin Immunol 2008; 129:90-102.
516 50. Fibbe WE, Hamilton MS, Laterveer LL, Kibbelaar RE, Falkenburg JH, Visser JW, et
517 al. Sustained engraftment of mice transplanted with IL-1-primed blood-derived stem cells. J
518 Immunol 1992; 148:417-21.
519 51. Garlanda C, Dinarello CA, Mantovani A. The interleukin-1 family: back to the future.
520 Immunity 2013; 39:1003-18.
521 52. McKinstry WJ, Li CL, Rasko JE, Nicola NA, Johnson GR, Metcalf D. Cytokine
522 receptor expression on hematopoietic stem and progenitor cells. Blood 1997; 89:65-71.
523 53. Yang J, Ikezoe T, Nishioka C, Nobumoto A, Yokoyama A. IL-1beta inhibits self-
524 renewal capacity of dormant CD34(+)/CD38(-) acute myelogenous leukemia cells in vitro and
525 in vivo. Int J Cancer 2013; 133:1967-81.
526 54. Yonemura Y, Ku H, Hirayama F, Souza LM, Ogawa M. Interleukin 3 or interleukin 1
527 abrogates the reconstituting ability of hematopoietic stem cells. Proc Natl Acad Sci U S A
528 1996; 93:4040-4.
529 55. Nagamachi A, Nakata Y, Ueda T, Yamasaki N, Ebihara Y, Tsuji K, et al. Acquired
530 deficiency of A20 results in rapid apoptosis, systemic inflammation, and abnormal
531 hematopoietic stem cell function. PLoS One 2014; 9:e87425.
532 56. Hahn KJ, Ho N, Yockey L, Kreuzberg S, Daub J, Rump A, et al. Treatment With
533 Anakinra, a Recombinant IL-1 Receptor Antagonist, Unlikely to Induce Lasting Remission in
534 Patients With CGD Colitis. Am J Gastroenterol 2015; 110:938-9.
535
536

Figure Legends

FIG 1. Increased HPC pool and HSC activation in X-CGD mice.

A-B, Number of LSK cells and FACS plots showing Lin^- cells from the BM of WT and X-CGD mice (n = 22). **C-E**, Frequency of myeloid progenitors, CMPs and GMPs in BM (n = 6). **F**, Colony formation by PB-derived cells (n = 18). **G**, Frequency of LSK cells in spleen (n = 9). **H-I**, Frequency of quiescent $Ki67^{neg}$ LSK SLAM cells from the BM and representative FACS plots showing the cell cycle distribution (n = 10). Error bars show mean ± SD. *, $p < 0.05$; **, $p < 0.01$.

FIG 2. X-CGD patients have fewer HSCs/HPCs in BM and PB.

A-B, Frequency of Lin^- $CD34^+CD38^{+/-}$ cells in the BM of aged-matched healthy controls (HC, n = 4) and X-CGD patients (n = 3) and representative FACS plots. **C-D**, Frequency of $CD34^+CD38^{+/-}$ cells and $CD34^+CD38^-CD90^+$ HSCs in G-CSF-mobilized PB mononuclear cells (n = 4). **E**, Representative FACS plots showing the distribution of HSCs/HPCs after 4 days culture of sorted PB $CD34^+CD38^{dim}CD90^+$ cells from one HC and two X-CGD patients. Error bars show mean + SD. *, $p < 0.05$.

FIG 3. HSCs/HPCs from X-CGD mice show faster exhaustion during hematopoietic reconstitution than WT cells.

A, Colony formation by BM cells after long-term culture ($n \geq 9$). **B**, Kaplan-Meier survival curves after serial 5-FU challenge (n = 6). **C**, Proportion of $eGFP^+$ and $tBFP^+$ donor-derived PB cells two to 18 weeks after competitive transplantation of gene-marked WT and X-CGD cells (n = 6). **D**, CRU assays with sorted HSCs. Shown is the frequency ± SE (n = 3). **E**, Percentage of multilineage reconstituted mice transplanted with BM cells obtained from D ($n \geq 14$). Data are provided as mean + SD. *, $p < 0.05$; **, $p < 0.01$; ***, $p < 0.001$.

562 **FIG 4. IL-1β is increased in the BM of X-CGD mice and induces HSC activation, HPC**
563 **expansion and reduces HSC long-term engraftment.**

564 **A**, IL-1β protein levels in bone lavages (n = 13). **B**, LSK cell frequency of IL-1β-treated WT
565 Lin^- cells (n = 6). **C-D**, Frequency of LSK cells and BrdU incorporation in LSK SLAM
566 $CD34^-$ cells in the BM of WT mice after IL-1β or PBS treatment (C: n = 7; D: n = 3). **E**, Cell
567 cycle distribution of LSK SLAM $CD34^-$ cells in IL-1β-treated WT and MyD88-deficient
568 mice (n = 3). **F-G**, Frequency of BM-derived CFUs and spleen LSK cells in IL-1β-treated
569 WT mice (n = 3). **H**, PB chimerism 16 weeks after competitive transplantation of cells from
570 IL-1β or PBS-treated animals (n = 4). Error bars show mean ± SD. *, $p < 0.05$; **, $p < 0.01$;
571 ***, $p < 0.001$.
572
573 **FIG 5. Blocking inflammatory signals restores HPC levels in X-CGD mice.**

574 **A-B**, Frequency of LSK cells in the BM (A) and spleen (B) of WT and X-CGD mice after
575 treatment with PBS or Anakinra (n = 3-4). **C-D**, Frequency of LSK cells in the BM (C) and
576 spleen (D) of X-CGD mice after treatment with PBS or Dexamethasone +/- Anakinra (n = 4).
577 **E**, IL-1b concentration in bone lavages from the mice in (C-D). Error bars show mean ± SD.
578 *, $p < 0.05$; **, $p < 0.01$. **D**, Proposed model of HSC/HPC exhaustion in X-CGD BM.
579

Figure No.1

Figure 1.

Click here to download Figure No.: Fig1-REVISED.pptx

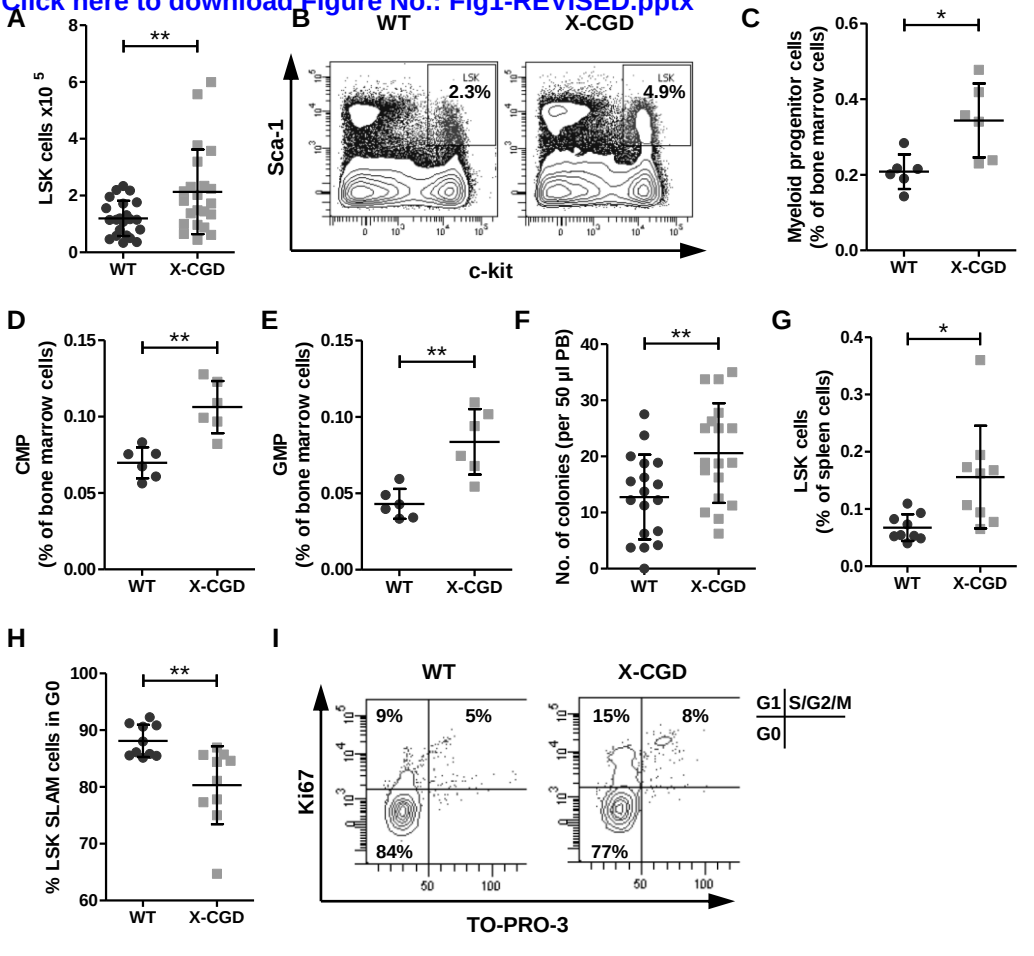

Figure No.2

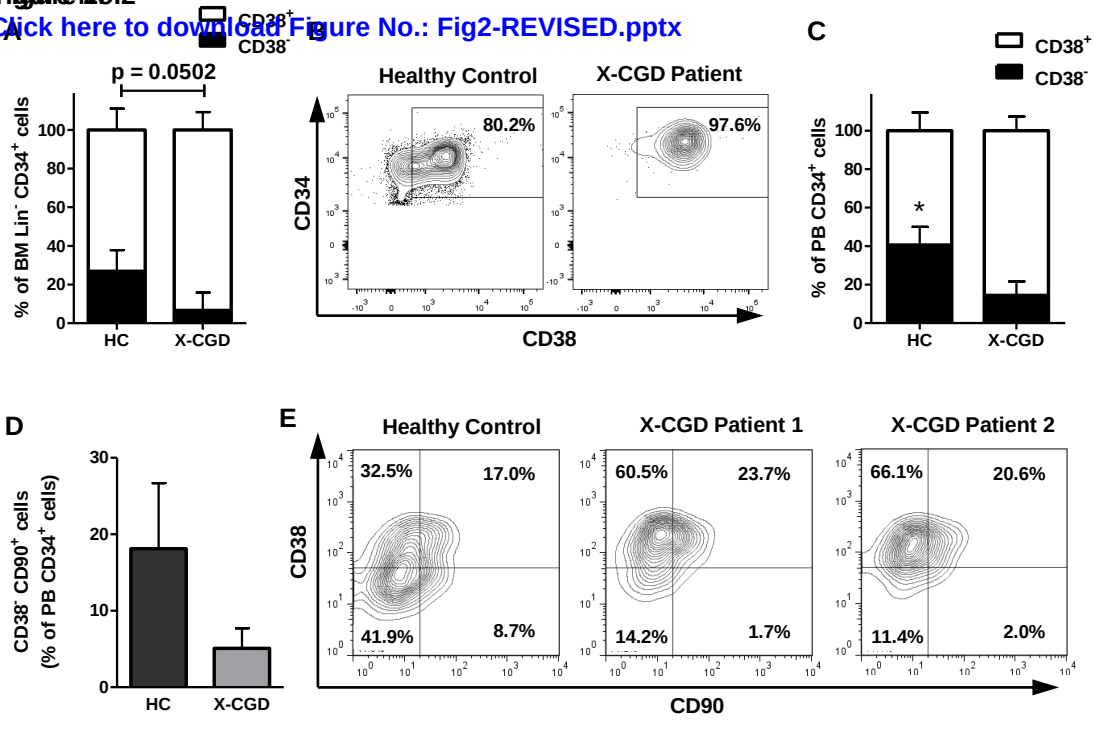

Figure No.3

Click here to download Figure No.: Fig3-REVISED.pptx

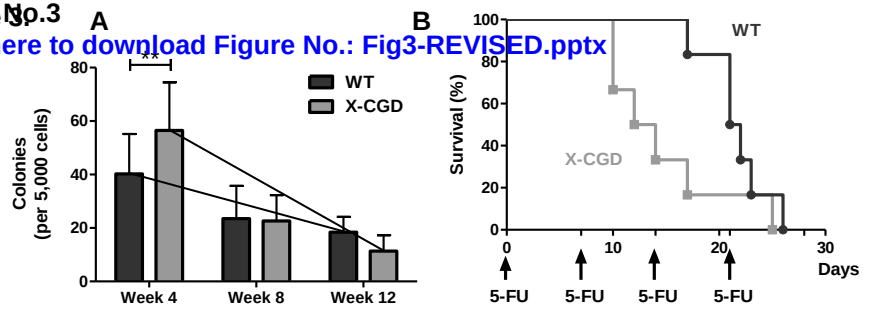

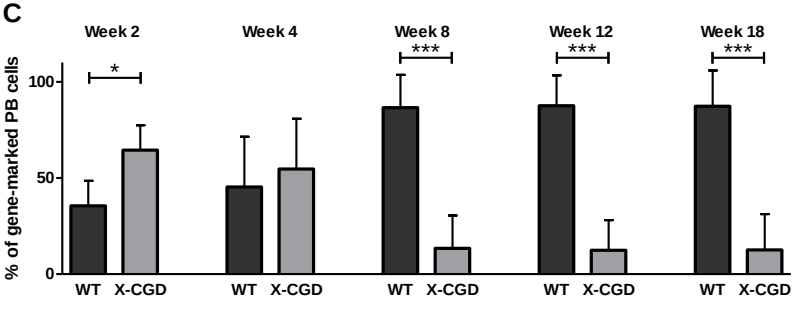

D

Competitive repopulation ability of LSK SLAM cells				
No. of Lin⁻ c-Kit⁺ Sca-1⁺ CD48⁻ CD150⁺ cells injected	No. of mice reconstituted/ tested (%) with WT cells		No. of mice reconstituted/ tested (%) with X-CGD cells	
2	1/13	(7.7)	1/15	(6.7)
10	4/14	(28.6)	1/12	(8.3)
50	12/15	(80.0)	8/11	(72.7)
250	14/15	(93.3)	9/11	(81.8)
CRU frequency:	**1 in 46** (1 in 35 – 1 in 59)		**1 in 85** (1 in 63 – 1 in 114)	

E

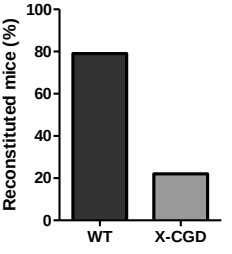

Figure No.4

Figure 4.

Click here to download Figure No.: Fig4-REVISED.pptx

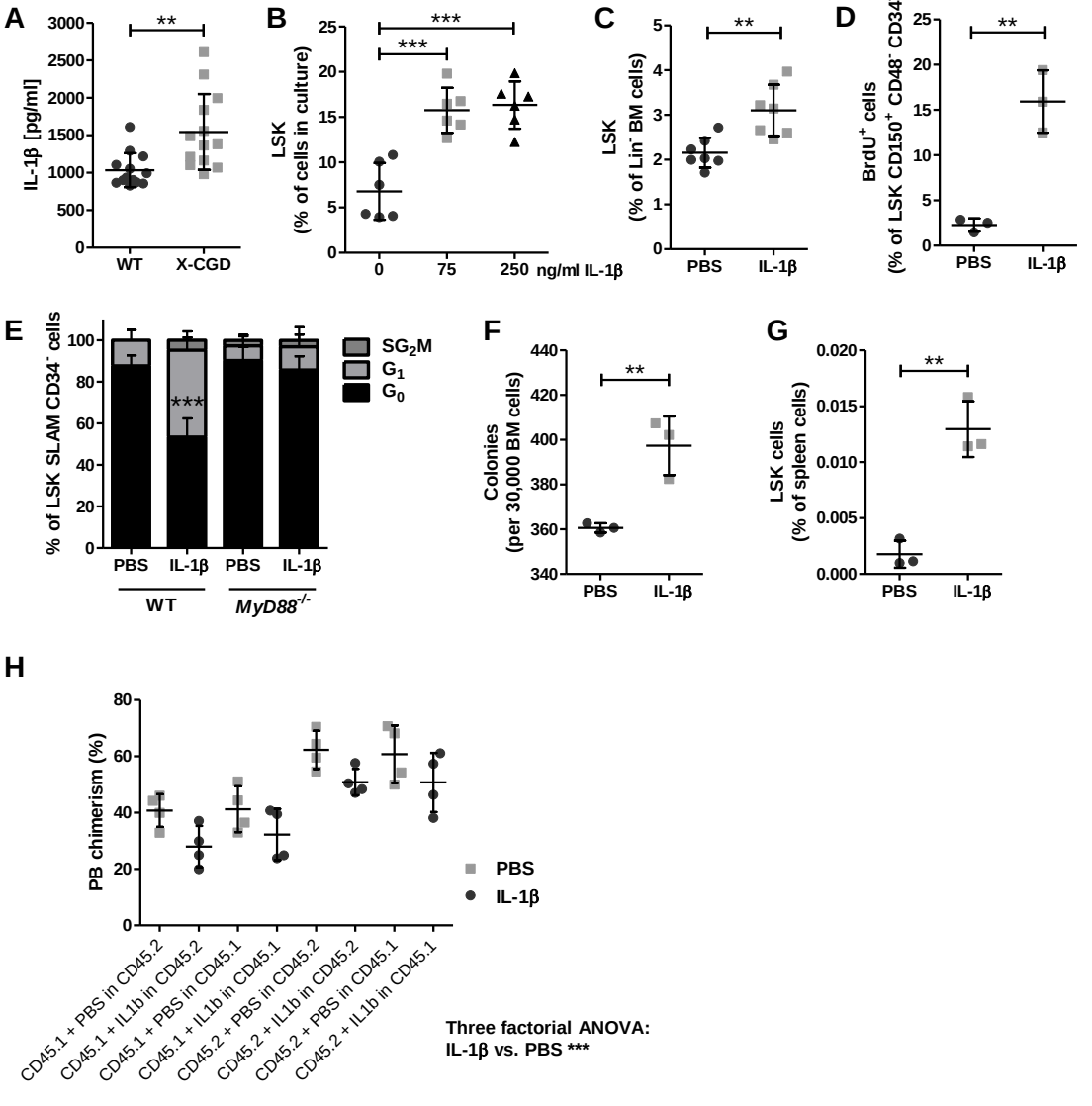

Figure No.5 - Unmarked

Figure 5.

Click here to download Figure No. - Unmarked: Figure 5 Revision_2.pptx

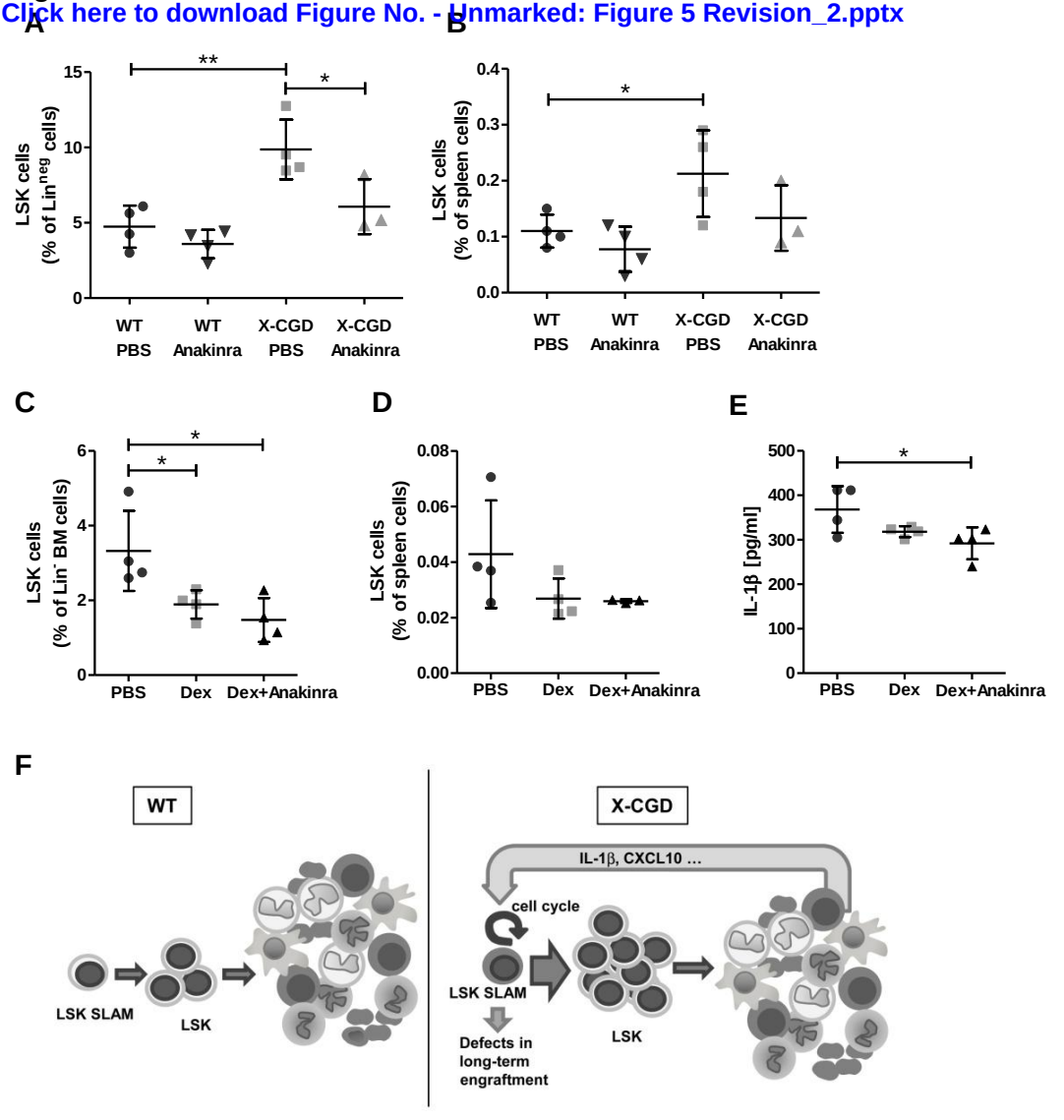

TABLE E1. Increased cytokine and chemokine levels in bone marrow fluid from X-CGD mice compared to WT controls as determined by protein arrays.

Cytokine / chemokine	Fold change X-CGD / WT	P-value*
CXCL9	7.8	0.046
CCL5	3.9	0.009
CXCL10	3.3	0.018
CXCL13	2.7	0.002
IL-1Ra	1.8	0.004
IL-1β	1.8	0.000
TREM-1	1.7	0.005
CCL2	1.6	0.000
CCL3	1.5	0.013
M-CSF	1.3	0.005
IL-3	1.2	0.039
TIMP-1	1.2	0.001
IL-1α	1.2	0.019
CXCL2	1.1	0.016
CCL4	1.1	0.001
IL-6	1.1	0.013
IL-5	1.1	0.030

*P values from unpaired two-tailed t-tests.

A

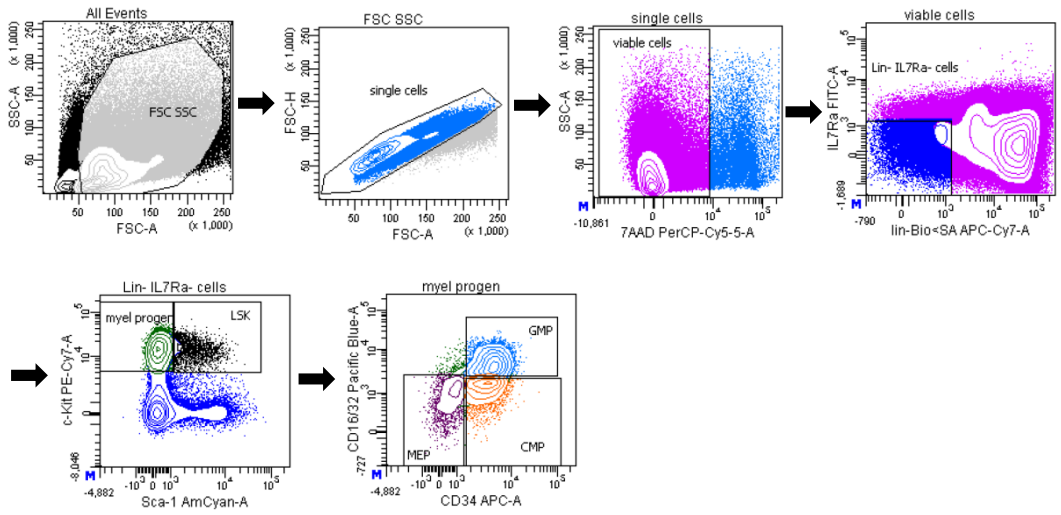

B

Markers for HSC/HPC subpopulations	
Cell population	Cell surface markers
Myeloid progenitors	Lin- IL7Ra- cKit+ Sca-1-
CMP	Lin- IL7Ra- cKit+ Sca-1- CD34+ CD16/32-
MEP	Lin- IL7Ra- cKit+ Sca-1- CD34- CD16/32-
GMP	Lin- IL7Ra- cKit+ Sca-1- CD34+ CD16/32+

C

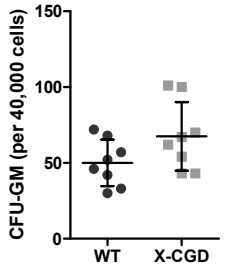

D

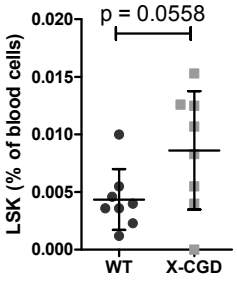

FIG E1. Analysis of the hematopoietic compartment in X-CGD and WT mice. **A**, Gating strategy used to identify HPC subpopulations in the bone marrow. **B**, Markers for myeloid progenitors, common myeloid progenitors (CMP), megakaryocyte-erythroid progenitors (MEP) and granulocyte-monocyte progenitors (GMPs) according to Challen et al., Cytometry A. 2009 Jan; 75(1):14-24. **C**, Number of CFU-GM in bone marrow samples from WT and X-CGD animals (n = 8). **D**, Frequency of LSK cells in peripheral blood of WT and X-CGD animals (n = 8). Statistical significance was calculated by unpaired two-tailed t-test.

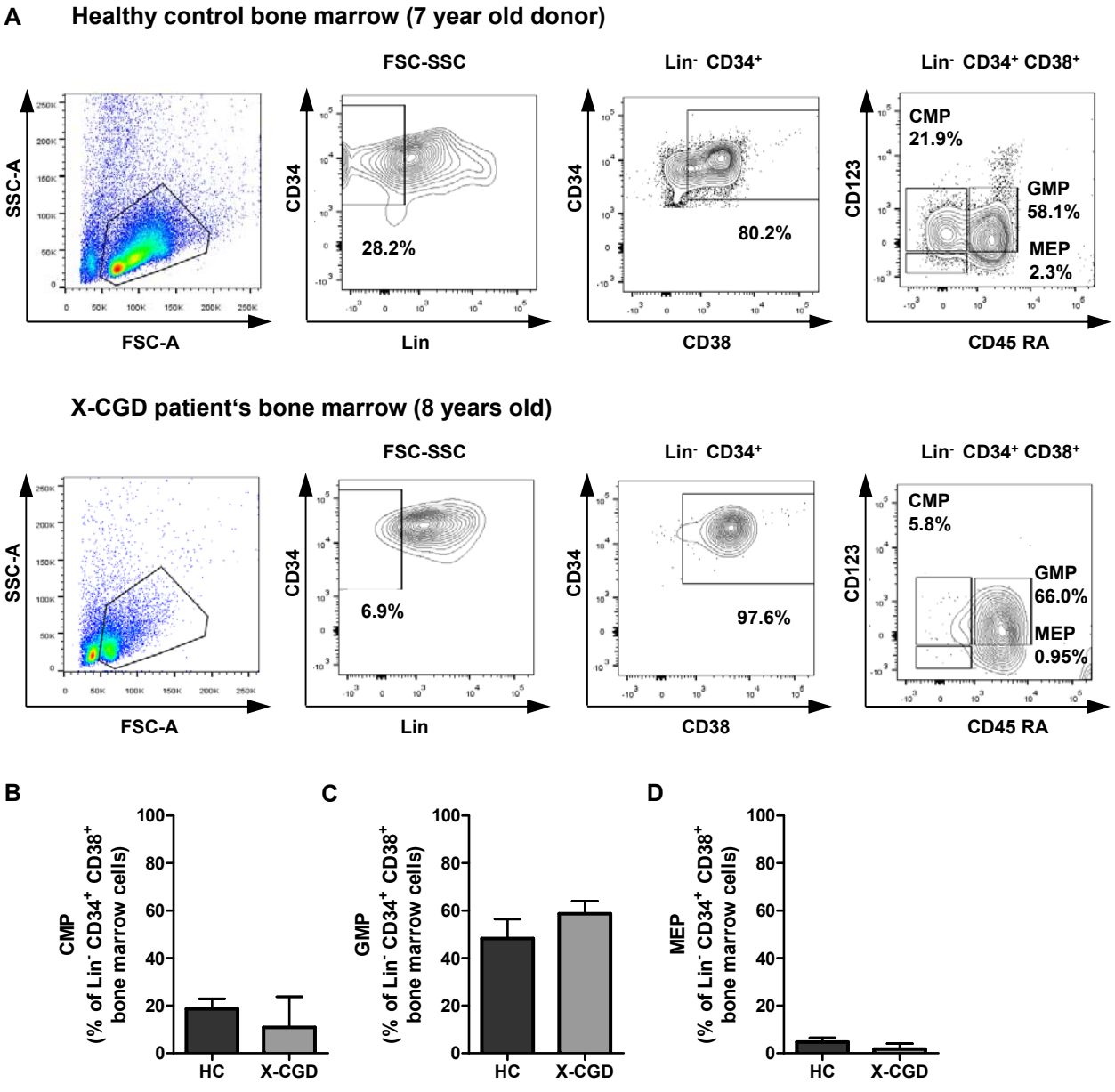

FIG E2. X-CGD patients have fewer HSCs/HPCs (CD38$^-$ CD34$^+$ Lin$^-$ cells) in the bone marrow and the distribution of CD38$^+$ CD34$^+$ Lin$^-$ committed progenitor cells differs from healthy controls. **A**, Representative FACS plots from bone marrow of a healthy donor and an aged-matched X-CGD patient showing the gating strategy to identify CMPs, GMPs and MEPs. HSCs/HPCs are within the CD38$^-$ CD34$^+$ Lin$^-$ population (gate not shown), while committed progenitors (CD38$^+$ CD34$^+$ Lin$^-$ cells) can be further separated into CMPs (CD38$^+$ CD34$^+$ Lin$^-$ CD123$^+$ CD45RA$^-$), GMPs (CD38$^+$ CD34$^+$ Lin$^-$ CD123$^+$ CD45RA$^+$) and MEPs (CD38$^+$ CD34$^+$ Lin$^-$ C123$^-$ CD45RA$^-$). **B-D**, Frequency of CMPs, GMPs and MEPs within the committed progenitor cell population in the bone marrow of X-CGD patients (n = 3) and age-matched healthy controls (HC) (n = 4) as determined by flow cytometry.

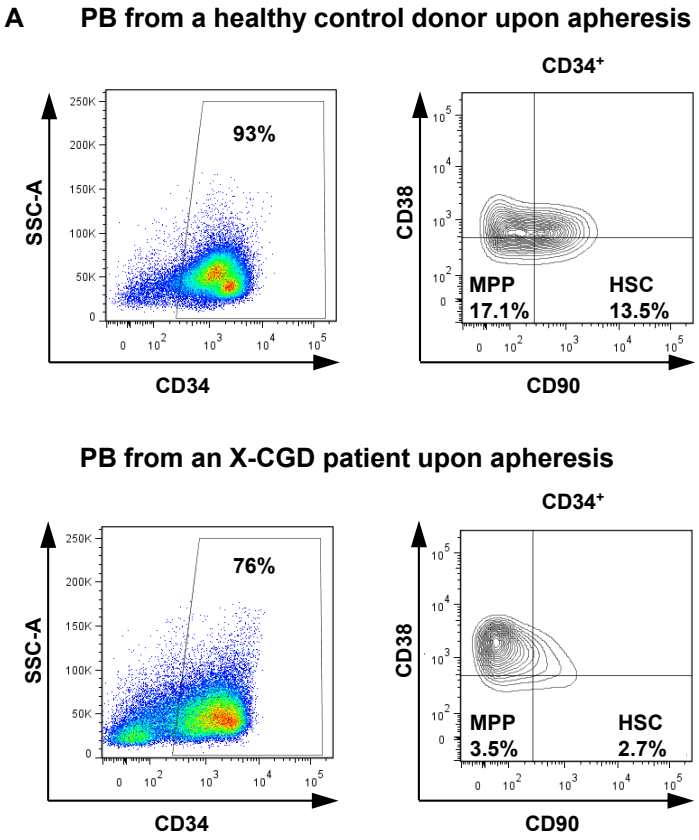

FIG E3. X-CGD patients contain less CD34$^+$ CD38$^-$ HSCs/HPCs in the peripheral blood (PB) upon apheresis than healthy controls. **A**, Representative FACS plots of G-CSF-mobilized PB mononuclear cells obtained from a healthy control (HC) and an X-CGD patient. HSCs are defined as CD34$^+$ CD38$^-$ CD90$^+$ cells.

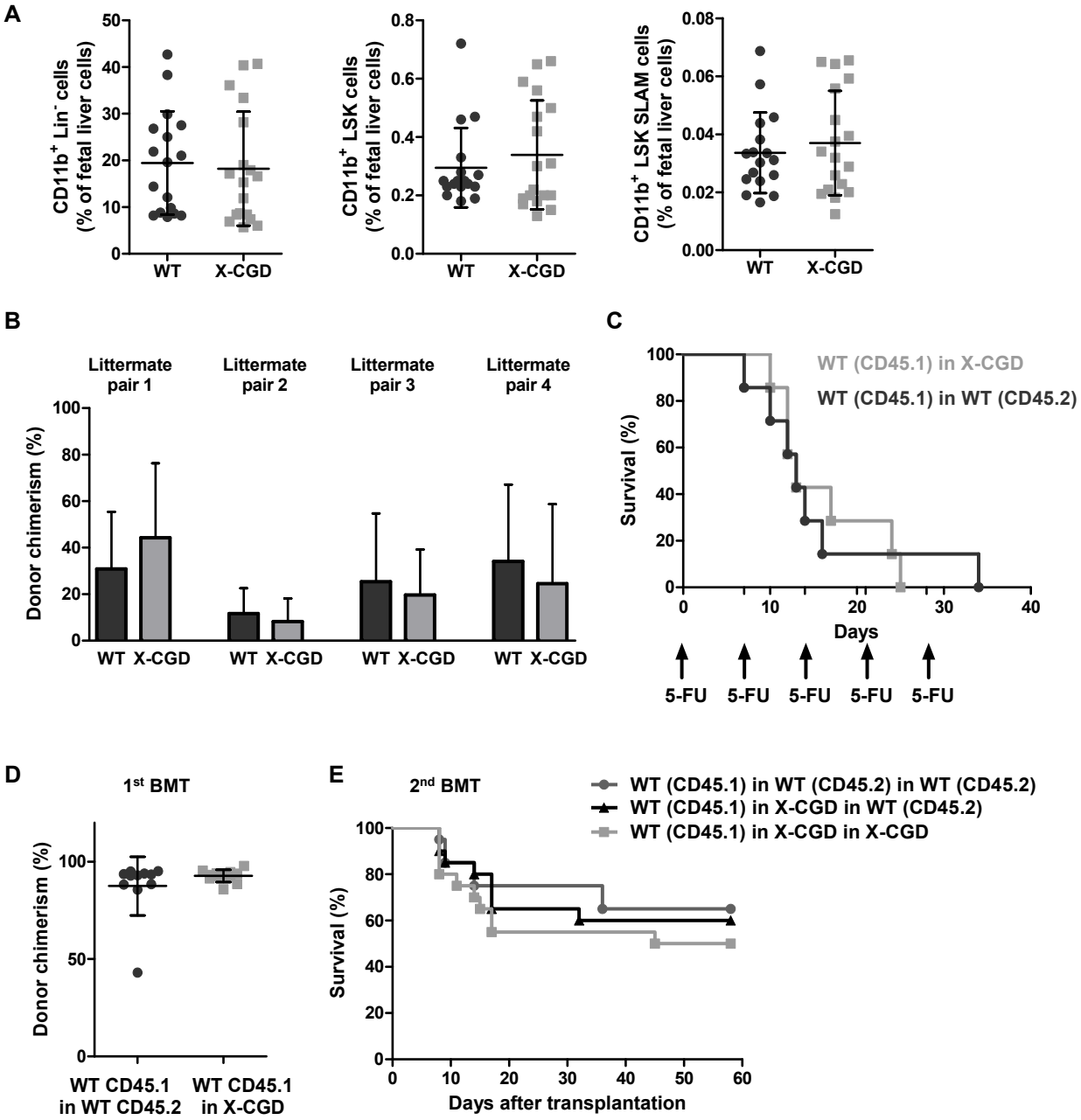

FIG E4. HSCs/HPCs from X-CGD fetal liver at E15.5 are present at the same frequencies and have the same reconstitution capacity as WT cells. **A**, Frequency of CD11b$^+$ Lin$^-$, CD11b$^+$ LSK and CD11b$^+$ LSK SLAM cells in the fetal liver of WT and X-CGD mice ($n \geq 17$). **B**, Competitive repopulation experiment using Lin$^-$ fetal liver cells from WT and X-CGD mice. The graphic shows exemplarily the result of PB reconstitution at week 16 after transplantation. **C-E**, X-CGD stromal cells are not impaired in their capability to support HSC functions. **C**, Survival of 5-FU-treated X-CGD or WT mice transplanted with WT (CD45.1) mononuclear cells ($n = 7$). **D**, Donor (CD45.1) chimerism in PB of transplanted WT and X-CGD mice 16 weeks after transplantation ($n \geq 11$). **E**, Kaplan-Meier survival curves of secondary hosts transplanted with mononuclear cells derived from the animals shown in 4D ($n = 20$). Error bars show SD.

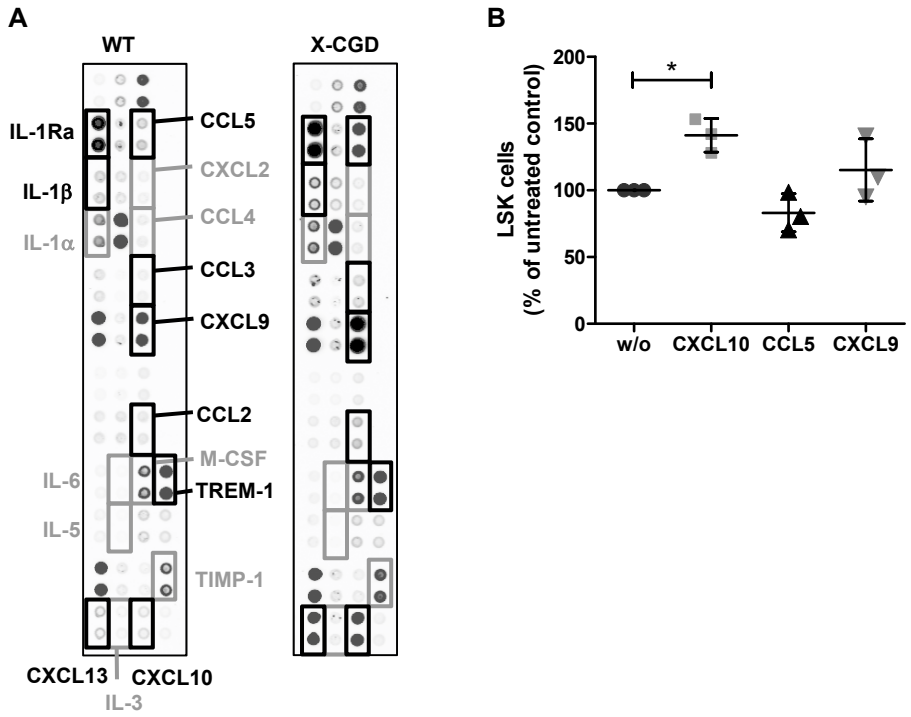

FIG E5. Cytokine levels are increased in bone lavages from X-CGD compared to WT mice and CXCL10 increases LSK cell frequency *in vitro*. **A**, Representative cytokine array using bone lavages from WT and X-CGD mice. Gray frames indicate significant differences ($p < 0.05$) between the littermate samples, black frames show cytokines upregulated ≥ 1.5-fold in X-CGD compared to WT lavages. Examination of the mice did not reveal any overt infections linked to these results. No differences in white blood counts ($16.0 \times 10^3/\mu l \pm 1.2$ vs. $14.0 \times 10^3/\mu l \pm 1.3$), PB lymphocyte counts ($11.8 \times 10^3/\mu l \pm 1.0$ vs. $9.7 \times 10^3/\mu l \pm 0.5$), or mean spleen weight (107 ± 5 mg vs. 110 ± 16 mg) were found for the WT versus X-CGD mice used for this analysis, respectively. **B**, LSK cell frequency of WT Lin^- cell after 3 days of culture with 250 ng/ml CXCL10, CCL5 or CXCL9 (n = 3). Statistical significance was analyzed by one-factorial ANOVA with Dunnet's Multiple Comparison Test. Error bars show mean ± SD. *, $p < 0.05$

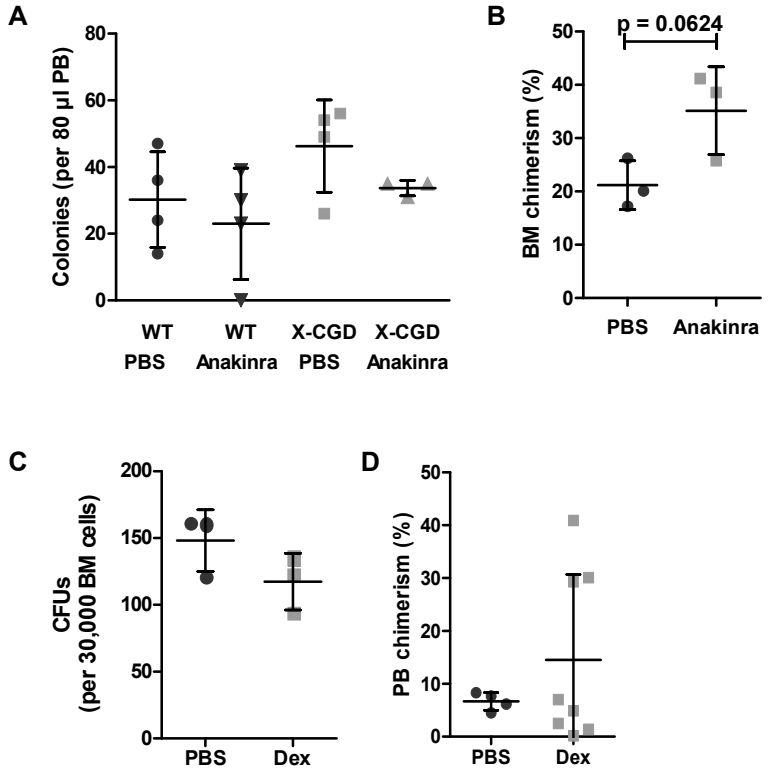

FIG E6. Blocking IL-1β signaling reduces the number of colony forming cells in bone marrow and peripheral blood, but has only minor effects on HSC engraftment.
A, WT and X-CGD mice were injected intraperitoneally with PBS or Anakinra (25 µg/g body weight) twice a day for 14-16 days and the frequency of colony-forming cells was measured in the peripheral blood (PB). **B,** Bone marrow (BM) chimerism in CD45.1 mice 19 weeks after transplantation of 4,000 Lin^- BM cells obtained from PBS- or Anakinra-treated X-CGD mice (CD45.2) together with 10^5 CD45.1 mononuclear competitor cells (n = 3). **C-D**, X-CGD mice were treated with Dexamethasone (Dex, 2 µg/g body weight) or PBS daily for 14 days. **C**, BM cells were assayed for the frequency of colony-forming units (CFUs) (n = 3). **D**, Lin^- BM cells from treated donors were used for competitive transplantation as described in (B). PB chimerism is depicted 8 weeks after transplantation ($n \geq 10$). Only animals with tri-lineage engraftment above 0.1% are shown. Error bars show mean ± SD.

Supplementary Data

Methods

Cell Isolation, Flow Cytometry and Cell Sorting.

For isolation of BM cells from mice humeri, tibiae, femurs and hips were dissected and flushed with PBS. Lineage depletion was performed with Lineage Cell Depletion Kit (MiltenyiBiotec, BergischGladbach, Germany) or Easy Sep Biotin Selection Kit (StemCell Technologies, Köln, Germany).For isolation of fetal liver HSCs the livers were dissected at E15.5 and triturated to single cell suspension. After genotyping, cells were incubated with biotinylated antibodies against CD3, CD19, B220, CD41, Gr-1 and Ter119 and lineage depleted like BM samples.

PB from tail vein was collected in EDTA tubes, underwent erythrocyte lysis (Pharm Lyse buffer, BD Biosciences, Heidelberg, Germany) and staining for flow cytometry. Spleen samples were prepared by mincing the organ through a cell strainer and erythrocyte lysis as described for PB.

For isolation of human $CD34^+$ cells we used the Lineage Cell Depletion Kit (MiltenyiBiotec) as recommended by the manufacturer. Aliquots were kept frozen in CryoStore freezing medium (StemCell Technologies) until use or analyzed immediately after isolation. Cells were analyzed and sorted on a FACSCanto II, LSR Fortessa and FACSAria (all: BD Biosciences) using the following antibodies: CD3 (500A2), human CD90 (5E10), human CD123 (7G3) (all: BD Biosciences), CD11b (M1/70), CD19 (eBio1D3), CD34 (RAM34), human CD34 (4H11), human CD38 (HIT2), CD41 (eBioMWReg30), CD45.1 (A20), human CD45RA (HI100), CD48 (HM48-1), CD127 (A7R34), B220 (RA3-6B2), c-Kit (2B8), Gr-1 (RB6-8C5), Sca-1 (D7), Ter-119 (all: eBioscience, Frankfurt, Germany), CD16/32 (93),

CD45.2 (104), CD150 (TC15-12F12.2) (all: BioLegend, Fell, Germany). Streptavidin eFluor450 was obtained from eBioscience. FACSDiva and FlowJo software were used for analysis.

Cell Cycle Analysis.

Ki67-FITC (clone B56) intracellular staining was performed according to BD Biosciences protocols, then cells were treated with RNase A (60 µg/ml) and stained with 0.5 µM TO-PRO-3 (both: Life Technologies, Darmstadt, Germany) or Hoechst33342 (Molecular Probes, Darmstadt, Germany). For IL-1β stimulation and *in vivo*BrdU-labeling mice received 2.5 µg IL-1β or PBS 20 h before BM harvest followed by BrdUintraperitoneally (18 mg/kg) 14 h before analysis. BrdU incorporation was detected using the FITC BrdU Flow Kit (BD Biosciences).

Colony Formation Assays.

CFU and long-term culture assays were performed according to the manufacturer's protocols using MethoCult GF M3434 and MyeloCult M5300 (both: StemCell Technologies).

5-FU Treatment of mice.

Weight-matched WT and X-CGD littermates or mice from WT (CD45.1) transplantations in WT (CD45.2) or X-CGD mice were injected weekly with 150 µg/g 5-fluorouracil (5-FU, Sigma-Aldrich, Taufkirchen, Germany). Neomycin (1.67 mg/ml) was added to drinking water. Mice were monitored and sacrificed in case of > 20% loss of body weight. Survival rates of the littermates were recorded.

Lentiviral Transduction.

Lentiviral vectors encoding for eGFP and tBFP were kindly provided by Christian Brendel, Georg-Speyer-Haus, Frankfurt. Vectors were produced as previously described.[E1]Transduction was performed as in Brendel et al.[E2], but cells were prestimulatedwith 300 ng/ml mSCF, 300 ng/ml mTPO, 100 ng/ml mFlt3-Ligand, 60 ng/ml mIL-3.

Transplantation of murine cells.

Lethally irradiated (9.5 Gy) mice were transplanted via tail vein injections. Unless stated otherwise, cells were transplanted into WT (CD45.1) mice. For CRU assays 2, 10, 50 or 250 sorted LSK SLAM cells were transplanted with 10^5 competitor mononuclear cells (MNCs) from WT (CD45.1) mice. PB of transplanted recipients was analyzed after 16 weeks by flow cytometry and mice with $\geq$ 1% donor-derived cells in the T-, B- and myeloid cell compartment were scored positive for donor cell engraftment. CRU frequency was calculated with the L-Calc software (Stem Cell Technologies). For secondary transplants, 10^5 BM MNCs from the first recipients transplanted with 50 or 250 LSK SLAM cells were transplanted with an equal number of WT (CD45.1) MNCs. Criteria for reconstitution were the same as above. For fetal liver experiments, 10^4 Lin^- fetal liver cells and 2 x 10^5 adult WT (CD45.1) MNCs were transplanted into irradiated WT (CD45.1) recipient mice.WT and X-CGD Lin^- fetal liver cells were obtained from littermate pairs. For assays with gene-marked cells, Lin^- cells from WT or X-CGD animals were transduced and 1:1 mixtures of transduced cells containing 70%-90% eGFP and tBFP-expressing cells were transplanted. For analysis of stromal cell effects, MNCs from WT (CD45.1) mice were transplanted into WT or X-CGD recipient mice. For 5-FU treatment, 5 x 10^5 WT (CD45.1) BM MNCs were injected and treatment was initiated 8 weeks after bone marrow transplantation (BMT). For serial BMTs

2 x 10^5 WT (CD45.1) BM MNCs were transplanted. After 16 weeks 2 x 10^5 BM MNCs from the first recipients were transplanted into secondary WT or X-CGD hosts. Survival rates of secondary recipients were monitored as during 5-FU treatment.

Cytokine Arrays and IL-1β ELISA.

BM lavage was obtained by flushing the hind limbs of WT and X-CGD mice with 0.5 ml PBS. Cells were removed by centrifugation and the lavage was frozen in aliquots at -80°C. BM lavage (0.35 ml) was used for the Proteome Profiler Mouse Cytokine Array Panel A (R&D Systems, Wiesbaden-Nordenstadt, Germany) according to the manufacturer's instructions and detected with the Odyssey Infrared Imaging System using IRDye 800CW Streptavidin. Signal quantification was performed with the Odyssey Application Software 2.1.12. Bone lavage samples were also analyzed with the RayBio Mouse IL-1β ELISA Kit (RayBiotech, Norcross, GA, USA) according to the manual.

Cytokine stimulation experiments

Sorted PB $CD34^+$, $CD38^{dim}$ and $CD90^+$ cells (500.000 cells/ml) were cultured in X-VIVO20 (Lonza, Walkersville, MD, USA), 1% HSA, hIL3 20ng/ml, hTPO 100ng/ml, hFlt-3L 300ng/ml, hSCF 300ng/ml for 4 days.

For the murine *in vitro* experiments 10^5 Lin^- cells were cultured in StemSpanSFEM (StemCell Technologies) + TPO + SCF (both 100 ng/ml), antibiotics and 75 ng/ml or 250 ng/ml IL-1β or 250 ng/ml CCL5, CXCL9 or CXCL10 (all: murine cytokines; PeproTech, Rocky Hill, NJ, US) or PBS. LSK cell frequency was determined after 3 days by FACS. For the *in vivo* experiments 250 ng IL-1β(LSK cells in BM, CFUs) or 2.5 µg IL-1β were injected into WT mice 12 h (LSK cells in BM, CFUs), 20 h (BrdU labeling and cell cycle analysis) or 44 h (LSK cells in spleen) prior to sacrifice. To analyze the effects of IL-1β treatment *in vivo*

on the engraftment capacity of HSCs upon transplantation, CD45.1 and CD45.2 WT mice were injected intraperitoneally with 250 ng IL-1β or PBS 5x every other day. Subsequently, MNCs were isolated and 2 x 10^6 MNCs from differently treated mice with distinguishable CD45 markers were mixedand transplanted into both CD45.1 and CD45.2 recipients. PB chimerism was analyzed 16 weeks after transplantation.

Anakinra and Dexamethasone treatment of mice

Anakinra (Kineret, SOBI, Stockholm, Sweden) treatment of X-CGD and WT mice consisted of two intraperitoneal injections per day at a concentration of 25 µg/g body weight for 14-16 days. Dexamethasone (Sigma-Aldrich) with/without Anakinra treatment of X-CGD mice was performed by daily intraperitoneal injections of 2 µg/g body weight Dexamethasone +/- 10 µg/g body weight Anakinra for 14 days. For subsequent BM transplantation, Lin^- cells were isolated from treated X-CGD mice and transplanted together with CD45.1 MNCs as competitors into CD45.1 WT recipients (4000 Lin^- cells + 10^5 MNCs per mouse). BM chimerism was detected 19 weeks after transplantation.

References

E1. Santilli G, Almarza E, Brendel C, et al. Biochemical correction of X-CGD by a novel chimeric promoter regulating high levels of transgene expression in myeloid cells. *Mol Ther*. 2011;19(1):122-132.

E2. Brendel C, Hanseler W, Wohlgensinger V, et al. Human miR223 promoter as a novel myelo-specific promoter for chronic granulomatous disease gene therapy. *Hum Gene Ther Methods*. 2013;24(3):151-159.